

DNS of compressible multiphase flows through the Eulerian approach

Matteo Cerminara

Scuola Normale Superiore di Pisa

Istituto Nazionale di Vulcanologia e Geofisica

Pisa, ITALY, matteo.cerminara@sns.it

Luigi C. Berselli

Dipartimento di Matematica

Università di Pisa

Pisa, ITALY, berselli@dma.unipi.it

Tomaso Esposti Ongaro

Istituto Nazionale di Geofisica e Vulcanologia

Section of Pisa

Pisa, ITALY, ongaro@pi.ingv.it

Maria Vittoria Salvetti

Dipartimento di Ingegneria Aerospaziale

Università di Pisa

Pisa, ITALY, mv.salvetti@ing.unipi.it

November 1, 2018

Abstract

In this paper we present three multiphase flow models suitable for the study of the dynamics of compressible dispersed multiphase flows. We adopt the Eulerian approach because we focus our attention to dispersed (concentration smaller than 0.001) and small particles (the Stokes number has to be smaller than 0.2). We apply these models to the compressible ($Ma = 0.2, 0.5$) homogeneous and isotropic decaying turbulence inside a periodic three-dimensional box (256^3 cells) using a numerical solver based

on the OpenFOAM® C++ libraries. In order to validate our simulations in the single-phase case we compare the energy spectrum obtained with our code with the one computed by an eighth order scheme getting a very good result (the relative error is very small $4 * 10^{-4}$). Moving to the bi-phase case, initially we insert inside the box an homogeneous distribution of particles leaving unchanged the initial velocity field. Because of the centrifugal force, turbulence induce particle preferential concentration and we study the evolution of the solid-phase density. Moreover, we do an *a-priori* test on the new sub-grid term of the multiphase equations comparing them with the standard sub-grid scale term of the Navier-Stokes equations.

1 Introduction

This work is part of a long-term project concerning modeling, simulation and analysis of particle-laden turbulent plumes, motivated by the study of the injection of ash plumes in the atmosphere during explosive volcanic eruptions. Ash plumes represent indeed one of the major volcanic hazards, since they can produce widespread pyroclastic fallout in the surrounding inhabited regions, endanger aviation and convect fine particles in the stratosphere, potentially affecting climate. Volcanic plumes are characterized by the ejection of a mixture of gases and polydisperse particles (ranging in diameter from a few microns to tens of millimetres) at high velocity (100-300 m/s) and temperature (900-1100 °C), resulting in an equivalent Reynolds number exceeding 10^7 (at typical vent diameters of 10-100 m) [12]. Estimates of the particle concentration in the plume [13] suggest that particle volume fraction decreases rapidly above the vent by the concurrent effect of adiabatic expansion of hot gases and turbulent entrainment of air, down to values below 10^{-3} , at which plume density becomes lower than atmospheric density.

To simulate such phenomenon by means of a fluid dynamic model, Direct Numerical Simulation (DNS) and a Lagrangian description of particles are beyond our current computational capabilities. Following [11], we therefore describe the eruptive mixture by adopting a multiphase flow approach, i.e., solid particles are treated as continuous, interpenetrating fluids (phases) characterized by specific rheological properties. For each phase, the Eulerian multiphase balance equations of mass, momentum and energy are considered. A Large Eddy Simulation (LES) framework, requiring the specification of sub-grid closure terms, is used to account for turbulence. Even by adopting such an approach, however, the description of a large number of Eulerian phases is still extremely computationally costly and has not allowed, so far, to perform reliable multiphase LES of volcanic plumes.

The aim of the present work is to formulate a faster, Eulerian multiphase flow model able to describe the most relevant non-equilibrium behaviour of volcanic mixtures (such as the effect of the grain-size distribution on mixing and entrainment, particle clustering and preferential concentration of particles by turbulence) while keeping the computational cost as low as possible, in order to achieve a sufficient resolution to perform reliable LES at the full volcanic scale.

In Section 2, we discuss a hierarchy of multiphase flow models, their potential and limits. Among them, a quasi-equilibrium model based on a first-order asymptotic expansion of model equations in powers of τ_s (the particle equilibrium time, [4]) is preferred in the context of volcanic plume simulations. Section 3 focuses on the capability of such models to describe gas-particle homogeneous and isotropic turbulence in compressible regime. Finally, we discuss the properties of the Favre-filtered models and the a-priori estimates of sub-grid terms, which is preliminary to the formulation of a closure model for LES of volcanic plumes.

2 Eulerian multiphase flow models

In order to use Eulerian models, we first discuss the physical constraints that characterized volcanic plumes. 1) Grain size distribution can be discretized into a finite number of particulate classes. 2) Particles are heavy, i.e., $\hat{\rho}_s/\hat{\rho}_g \gg 1$ ($\hat{\rho}_s \approx 400 - 3000 \text{ kg/m}^3$), where the hat denotes the density of the phase material. 3) Each class can be described as a continuum (Eulerian approach), i.e., the mean free path is much smaller than, say, the numerical grid size). 4) Low concentration: particle volume fraction $\varepsilon_s = V_s/V < 10^{-3}$. Under such conditions, particles can be considered as non-interacting (pressure-less) or weakly-interacting (small pressure term). As a consequence of 2) and 4), the bulk densities ($\rho_g = (1 - \varepsilon_s)\hat{\rho}_g$ and $\rho_s = \varepsilon_s\hat{\rho}_s$) can be of the same order of magnitude (about 1 kg/m^3 or less).

Following the same approach described in [1], we can build a hierarchy of models based on the ratio between a particle characteristic equilibrium time τ_s and a characteristic time of the fluid flow τ_η (which can be the Kolmogorov time in the case of developed turbulent flows, or a large eddy turnover time).

Moreover, to simplify our analysis, we will assume in the following that the flow is iso-entropic (i.e., we neglect the initial explosive phase, which affects only the first hundreds of metres above the vent), and we consider a barotropic model, thus avoiding to solve the full energy equation. This approach is widely used in atmospheric and plume models and verified by experiments [8, 13].

Barotropic Eulerian-Eulerian model: For small relative Reynolds number, $\rho_g|\mathbf{u}_s - \mathbf{u}_g|d_s/\mu < 1$ (where d_s is the particle's diameter, μ and ρ are gas density and dynamic viscosity and \mathbf{u}_g and \mathbf{u}_s are the gas and solid phase velocities) the

drag force between the gas and a solid phase can be expressed by the Stokes law $\mathbf{f}_d = \rho_s(\mathbf{u}_s - \mathbf{u}_g)/\tau_s$ and particle relaxation time is defined by $\tau_s = \hat{\rho}_s d_s^2 / 18\mu$.

When τ_s is of the same order of magnitude as τ_η , the fully coupled multiphase flow equations must be considered. For a two-phase (monodisperse) mixture, the system of mass and momentum balance equations reads:

$$\partial_t \rho_g + \nabla \cdot (\rho_g \mathbf{u}_g) = 0, \quad \partial_t \rho_s + \nabla \cdot (\rho_s \mathbf{u}_s) = 0, \quad (1)$$

$$\partial_t (\rho_g \mathbf{u}_g) + \nabla \cdot (\rho_g \mathbf{u}_g \otimes \mathbf{u}_g + p_g \mathbf{I}) - \nabla \cdot \boldsymbol{\sigma} = \frac{\rho_s}{\tau_s} (\mathbf{u}_s - \mathbf{u}_g) + \rho_g \mathbf{g}, \quad (2)$$

$$\partial_t (\rho_s \mathbf{u}_s) + \nabla \cdot (\rho_s \mathbf{u}_s \otimes \mathbf{u}_s + p_s \mathbf{I}) - \nabla \cdot \boldsymbol{\pi} = -\frac{\rho_s}{\tau_s} (\mathbf{u}_s - \mathbf{u}_g) + \rho_s \mathbf{g}, \quad (3)$$

where the subscripts g and s represent the gas and solid phase, respectively, the pressure terms p_s and p_g are given by the barotropic model as $p = p_0(\rho/\rho_0)^\gamma$ (but the exponent γ may be different), $\boldsymbol{\pi} = \mu_s \rho_s \nabla^{\text{sym}} \mathbf{u}_s$, $\boldsymbol{\sigma} = \mu (\nabla^{\text{Sym}} \mathbf{u}_g - \frac{2}{3} \nabla \cdot \mathbf{u}_g \mathbf{I})$ and $\gamma(\gamma_s)$ is the specific heat ratio of the gaseous (solid) phase. Here \mathbf{g} is the gravitational acceleration, which has not been considered in the following simulations.

Fast Eulerian model: for smaller (but non negligible) τ_s , it is possible to insert a first-order approximation of the particle velocity into the Eulerian-Eulerian equations: $\mathbf{u}_s = \mathbf{u}_g - \tau_s \mathbf{a}_g$, where $\mathbf{a}_g = \frac{D}{Dt}(\mathbf{u}_g) - \mathbf{g}$ is the gas phase acceleration (cf. [4]).

This allows to reduce the number of model equations to one single momentum equation for the mixture plus N equations for mass conservation. By assuming also local thermal equilibrium, we get the following system, again written for a two-phase mixture for the sake of simplicity (here $\rho_m \equiv \rho_g + \rho_s$):

$$\partial_t \rho_g + \nabla \cdot (\rho_g \mathbf{u}_g) = 0, \quad \partial_t \rho_s + \nabla \cdot (\rho_s \mathbf{u}_s) = 0, \quad (4)$$

$$\partial_t (\rho_m \mathbf{u}_g) + \nabla \cdot (\rho_m \mathbf{u}_g \otimes \mathbf{u}_g + p \mathbf{I}) - \nabla \cdot \boldsymbol{\sigma} = \rho_m \mathbf{g} + \tau_s \nabla \cdot (\rho_s \mathbf{a}_g) \mathbf{u}_g. \quad (5)$$

Dusty Gas model: Finally, when τ_s is negligible, the fast Eulerian model reduces to the so-called dusty-gas model [7], in which all phases have the same velocity. As predicted by the theory, preliminary simulations carried out for turbulent plumes have shown that the dusty-gas model is not capable of reproducing preferential concentration and the effect of particle inertia on turbulent mixing. Therefore, such a model does not appear to be well suited to our purposes, and, hence, the results of the dusty-gas model will not be shown herein.

We implemented these models into OpenFOAM®. Since the flow density is varying in time and space due to the presence of particles, we adopted a robust numerical scheme to simultaneously treat compressibility, buoyancy effects, and turbulent dispersal dynamics, which is based on a segregated solution algorithm [5], with an adaptive time-stepping. Since we limit our analysis to moderate Marms (up to 0.6), we do not need shock-capturing schemes. Here $(\cdot)_{\text{rms}}$ stands for root mean square.

3 Numerical results

As a first step for the appraisal of the considered models, we performed numerical tests by performing DNS of decaying homogeneous isotropic turbulence as reported in [6, 9]. We consider an initial solenoidal velocity field with spectrum $E(k) \propto (k/k_0)^4 \exp(-2(k/k_0)^2)$, $k_0 = 2$ and viscosity $\mu \simeq 0.00239$ to have the Taylor microscale $\lambda = 1/2$, $Re_\lambda = 50$ and that the Kolmogorov scale η remains bigger than the mesh-size: $\eta/\Delta x \geq 2.0$. The initial velocity field is identical for both the gas and the solid, the Stokes number at $t = 0$ is $St = 0.02$, the specific-heat ratios are $\gamma = 1.4$ and $\gamma_s = 1$ and the solid phase viscosity $\mu_s = 10^{-8}$. Since $\rho_s = \rho_g = 1$, the inertial forces of particles are significant in the flow dynamics.

To validate our simulations in the single-phase case, we compared the energy spectrum obtained with our code with the one computed by an eighth order scheme [10]. The comparison is made after one large-eddy turnover time at $Ma_{rms} = 0.2$, we find the L^2 norm of the difference between the two spectra is $4.0 * 10^{-4}$ (cf. Fig. 1). This validates the accuracy of our numerical solver in the single-phase case.

As in [6], we keep the same velocity field in all simulations and modified the initial homogeneous pressure field in order to modify the Mach number. In the single-phase case we used $Ma_{rms} = 0.2, 0.5$. In Fig. 1 we compare the two resulting energy spectra. In the gas-particle case, we keep the same velocity and pressure fields, modifying in this way the non dimensional parameters. In particular the equivalent Reynolds number doubles because the mixture bulk density moves from $\rho_g = 1$ to $\rho_g + \rho_s = 2$, while the equivalent Mach number increases of a factor $\simeq 1.4$ because the speed of sound of the mixture decreases.

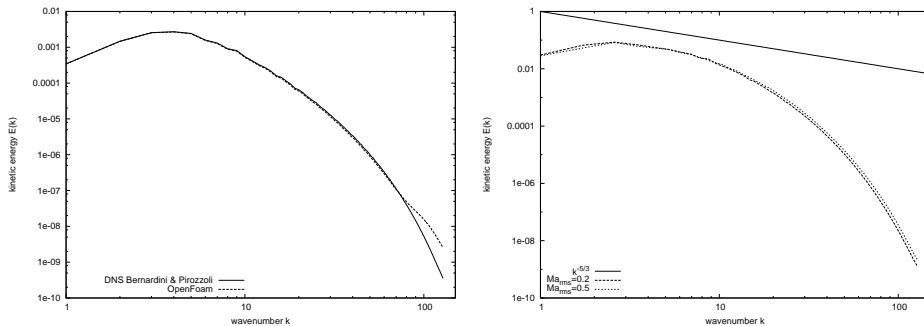


Figure 1: Comparison of the Energy spectrum: PISO vs. eight order DNS (see [10]) after one large-eddy turnover time (left). PISO at $Ma_{rms} = 0.2, 0.5$ after two large-eddy turnover time (right).

Comparison of the two Eulerian models: Fig 2 shows the time evolution of kinetic energy and enstrophy obtained in the single-phase case (NSE) and in the

two-phase one by the barotropic Eulerian and fast Eulerian models respectively. We first observe that, as expected because of the doubled Re, the vorticity and

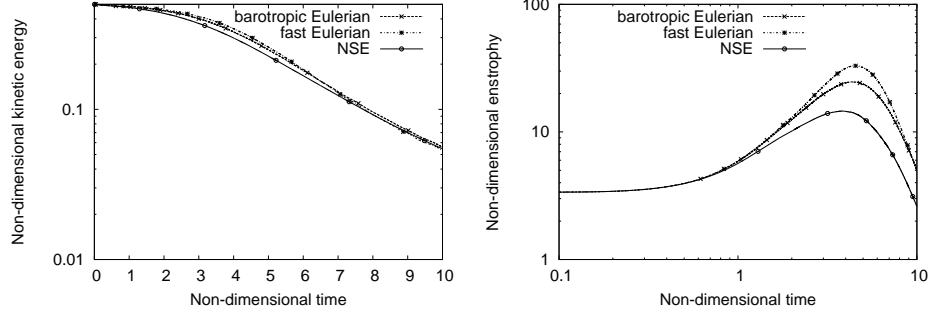


Figure 2: Turbulence global properties evolution: Kinetic energy (left) and Enstrophy (right) .

the energy are larger than in the single-phase case. Next, we observe that in our codes the Fast Eulerian model is less diffusive than the Eulerian one (the enstrophy becomes larger and the turbulent dissipation is more efficient, cf. [6]). This fact is qualitatively observable also in Fig. 3, where we show isosurfaces of the solid density for the two Eulerian models. In Fig. 4 we report the evolution of the

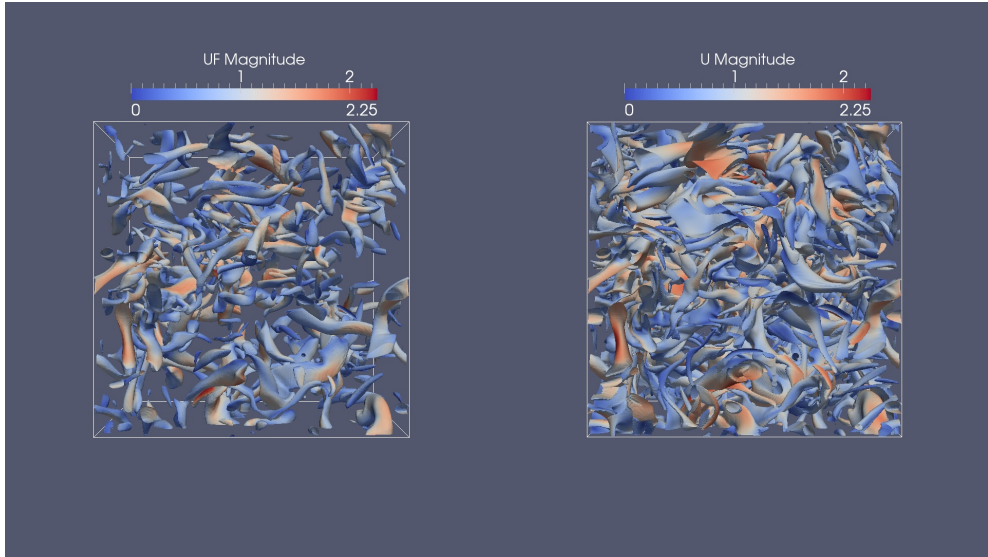


Figure 3: Isosurfaces of the solid phase density: barotropic Eulerian (left) and fast Eulerian (right). Turbulence induces particle preferential concentration.

density fluctuations, for both the solid and gaseous phases. We find that the presence of a massive solid phase increases the density fluctuation (the Mach number

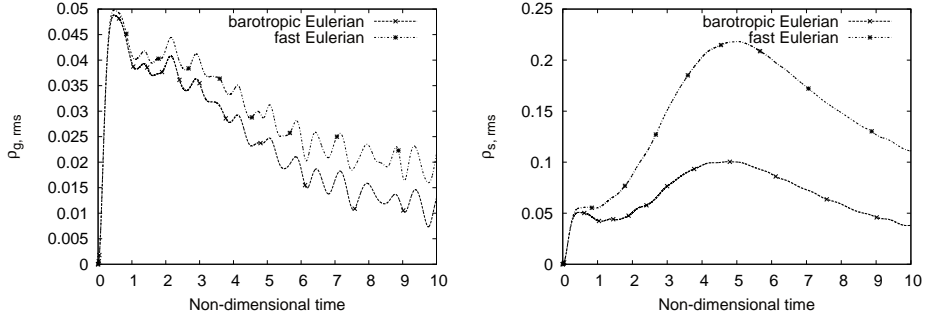


Figure 4: Density fluctuations $\sqrt{\langle (\rho - \langle \rho \rangle)^2 \rangle}$: Gaseous phase ρ_g (left), solid phase ρ_s (right).

is modified by the presence of a solid phase), and that in the Fast Eulerian model the preferential concentration of the solid particles is stronger than in the Eulerian simulation (the latter being more diffusive than the former). These differences between the two models are quite surprising since for the values of the Stokes number of the considered particles they are expected to give close results. A possible cause may be a difference in the treatment of source term in the two Eulerian models. In particular, the Stokes coupling between the two phases has been treated explicitly in the Eulerian model, probably underestimating its fluctuations. This will be further investigated in future works.

A priori tests: Moving forward, we use the DNS results to evaluate the SGS terms which would arise in LES. To filter model equations, we have defined a Favre filter $\tilde{\cdot}$, $\check{\cdot}$, for each phase so that: $\overline{\rho_g \psi} = \tilde{\rho}_g \tilde{\psi}$ and $\overline{\rho_s \psi} = \check{\rho}_s \check{\psi}$. Using these filters in our models we get new sub-grid terms, which are evaluated on the DNS results.

In the barotropic Eulerian model, the SGS terms different from zero are:

$$E_1 = \nabla \cdot \tau, \quad E_2 = \nabla \cdot \theta, \quad E_3 = \overline{\rho_s}(\check{\mathbf{u}}_g - \tilde{\mathbf{u}}_g)/\tau_s, \quad E_4 = a \nabla(\overline{\rho_g^\gamma} - \overline{\rho_g}^\gamma),$$

where $a = p_0/\rho_0^\gamma$, $\tau = \bar{\rho}_g(\mathbf{u}_g \widetilde{\otimes} \mathbf{u}_g - \tilde{\mathbf{u}}_g \otimes \tilde{\mathbf{u}}_g)$, and $\theta = \bar{\rho}_s(\mathbf{u}_s \widetilde{\otimes} \mathbf{u}_s - \check{\mathbf{u}}_s \otimes \check{\mathbf{u}}_s)$. The subgrid terms E_1 and E_2 represent the divergence of the classical SGS stress tensor for the gas and the solid phases respectively, while E_3 represents the SGS effects on the Stokes drag acting on the particles and E_4 the barotropic pressure SGS term. Figure 2 shows the time evolution of the r.m.s. of E_i in semi-log scale. The filtering is made by a top hat filter with radius $\delta = \sqrt{2}h$.

We observe that the subgrid term related with the barotropic pressure is significantly smaller than the others. Hence, in addition to the terms present in the mono-phase case, also the Stokes force of interaction between the two phases is of the same order of magnitude and requires LES modeling.

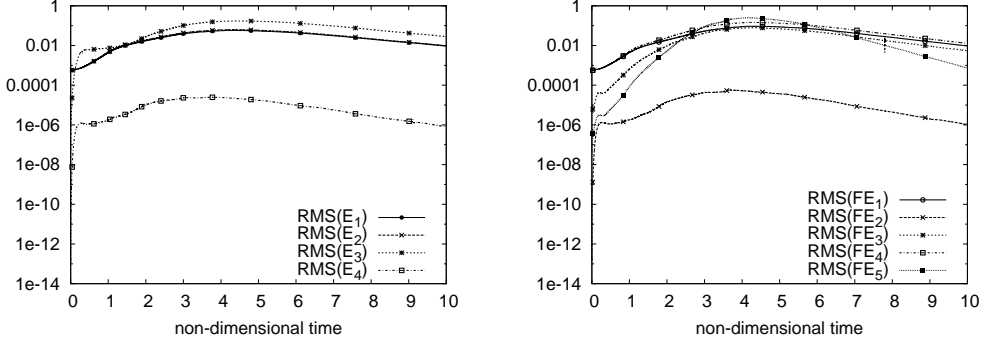


Figure 5: Barotropic Eulerian: Evolution of the RMS of E_i at Mach=0.35 (left), Barotropic Fast Eulerian: Evolution of the RMS of FE_i at Mach=0.28 (right).

In the case of the Fast Eulerian model, different terms comes out from the Favre filtering operation. In particular, we have:

$$\begin{aligned} FE_1 &= \nabla \cdot \bar{\rho}_g (\widetilde{\mathbf{u}_g \otimes \mathbf{u}_g} - \tilde{\mathbf{u}}_g \otimes \tilde{\mathbf{u}}_g), \quad FE_2 = \bar{p} - p_0 (\bar{\rho}_g / \rho_0)^\gamma, \\ FE_3 &= \partial_t (\bar{\rho}_s (\tilde{\mathbf{u}}_g - \tilde{\mathbf{u}}_g)), \quad FE_4 = \nabla \cdot \bar{\rho}_g (\mathbf{u}_g \check{\otimes} \mathbf{u}_g - \tilde{\mathbf{u}}_g \otimes \tilde{\mathbf{u}}_g), \\ FE_5 &= \tau_S \left[\nabla \cdot (\rho_s \mathbf{a}_g) \mathbf{u}_g - \nabla \cdot (\bar{\rho}_s \tilde{\mathbf{a}}_g) \tilde{\mathbf{u}}_g \right] \end{aligned}$$

As in the other case the subgrid term related with the barotropic pressure is significantly smaller than the others. The other terms require LES modeling and we can observe that they are of the same order of magnitude of the relevant terms appearing in the Eulerian case.

4 Conclusions

We performed DNS of multiphase flows comparing results between the barotropic Eulerian and the fast Eulerian model. Clearly the fast Eulerian one is less time consuming (about a factor one half), but it seems that at least in our setting the overall quality of the numerical results is still acceptable. The fast Eulerian model seems to be less diffusive and consequently the preliminary results concerning the preferential concentration are slightly better. A conclusive assessment requires comparison with Lagrangian simulations (as those in [2]), which we do not have currently at disposal, due to the peculiarity of the large initial solid phase inertia. Further tests are ongoing with the objective of well reproducing with LES both turbulence and preferential concentration for poly-disperse mixtures.

References

- [1] Balachandar, S., Eaton, J. K. Turbulent Dispersed Multiphase Flow. *Ann. Rev. Fluid Mech.* **42**, 111–133 (2010).
- [2] Boffetta, G., Celani, A., De Lillo F., Musacchio, S., The Eulerian description of dilute collisionless suspension. *Europhysics Letters* **78**, 14001 (2007).
- [3] Cerminara, M., Berselli, L.C., Esposti Ongaro, T. & Salvetti, M.V., Movie of the multiphase homogeneous and isotropic turbulence modelled with the barotropic Eulerian-Eulerian model vs the fast-Eulerian model, (2013). <http://youtu.be/zRC65P8MdKA>
- [4] Ferry, J., Balachandar, S., A fast Eulerian method for disperse two-phase flow *Int. J. Multiphase Flow* **27**, 1199–1226 (2001).
- [5] Demirdzic, I., Lilek, Z. & Peric, M., A collocated finite volume method for predicting flows at all speeds. *Int. J. Numer. Methods Fluids*, **16**, 1029–1050, (1993).
- [6] Garnier, E., Mossi, M., Sagaut, P., Comte, P., Deville, M. On the Use of Shock-Capturing Schemes for Large-Eddy Simulation. *J. Comput. Physics* **153**, 273–311 (1999).
- [7] Marble, F.E., Dynamics of Dusty Gases. *Ann. Rev. Fluid Mech.* **2**, 397–446 (1970).
- [8] Morton, B. R, Taylor, G., Turner J. S., Turbulent Gravitational Convection from Maintained and Instantaneous Sources, *Proc. R. Soc. Lond. A* **234**, 1–23 (1956).
- [9] Lesieur, M., Métais, O. & Comte, P., Large-Eddy Simulations of Turbulence. *Cambridge University Press*, New York (2005).
- [10] Pirozzoli, S. Grasso, F., Direct numerical simulations of isotropic compressible turbulence: Influence of compressibility on dynamics and structures, *Phys. Fluids* **16**, 4386 (2004).
- [11] Esposti Ongaro, T., Cavazzoni, C., Erbacci, G., Neri, A., Salvetti, M.V., A parallel multiphase flow code for the 3D simulation of explosive volcanic eruptions, *Par. Comp.* **33**, 541–560 (2007)

- [12] Valentine, G. A., Eruption column physics. *From Magma to Tephra: Modelling Physical Processes of Explosive Volcanic Eruptions* (edited by A. Freudent and M. Rosi). Elsevier, New York, 91–136 (2001).
- [13] Woods A.W., The fluid dynamics and thermodynamics of eruption columns. *Bull. Volcanol.* **50**, 169–193 (1988).